Ecological Modelling 409 (2019) 108745

Contents lists available at ScienceDirect

Ecological Modelling

journal homepage: www.elsevier.com/locate/ecolmodel

Modelling the multi-scaled nature of pest outbreaks

Matthias Wildemeersch[a,*], Oskar Franklin[a], Rupert Seidl[b], Joeri Rogelj[a], Inian Moorthy[a], Stefan Thurner[c,a,e,d,f]

[a] International Institute for Applied Systems Analysis, Laxenburg A2361, Austria
[b] University of Natural Resources and Life Sciences, Peter Jordan Straße 82, A-1190 Vienna, Austria
[c] Section for Science of Complex Systems, Medical University of Vienna, Spitalgasse 23, A-1090 Vienna, Austria
[d] Santa Fe Institute, 1399 Hyde Park Road, Santa Fe, NM 87501, USA
[e] Complexity Science Hub Vienna, Josefstädter Straße 39, A-1080 Vienna, Austria
[f] Complexity Institute, Nanyang Technological University, Nanyang Drive 18, 637723, Singapore

ARTICLE INFO

Keywords:
Landscape management
Network of networks
Pest dynamics
Pest outbreaks

ABSTRACT

Recent research suggests that the spread of pest outbreaks is driven by ecological processes acting at different spatial scales. In this work, we establish a network model for the analysis and management of pest outbreaks that takes into account small-scale host-pest interactions as well as landscape topology and connectivity. The model explains outbreak cycles both for geometrid moths and bark beetles, and provides insight into the relative importance and interactions between the multi-scale drivers of outbreak dynamics. Our results demonstrate that outbreak behavior is most sensitive to changes in pest pressure at the local scale, and that accounting for the spatial connectivity of habitat patches is crucial to capturing the spreading behavior through landscapes. In contrast to early warning signals based on retrospective data, our model provides predictions of future outbreak risk based on a mechanistic understanding of the system, which we apply for landscape-scale forest management.

1. Introduction

Pest outbreaks can strongly affect ecosystem health, and hence have far-reaching consequences for local economies that depend on specific ecosystem services (Ludwig et al., 1978; Lewis et al., 2010; Fahse and Heurich, 2011; Nelson et al., 2013). It has become clear in recent research that pest outbreaks are more complex than previously assumed. Specifically, outbreaks are driven by factors on multiple scales, i.e., host abundance at the stand level, connectivity at the landscape level, and climate related effects at the regional level (Senf et al., 2017; Seidl et al., 2016b; Raffa et al., 2008; Peters et al., 2004; With and Crist, 1995). These insights coincide with a global increase in disturbances by forest pests, inter alia influenced by anthropogenic climate change (Seidl et al., 2017, 2014; Kautz et al., 2017). Empirical evidence supports the relevance of these multiple factors, but an integrated understanding of their respective roles, their interactions, and the resulting complex dynamics is still missing, limiting our ability to predict pest outbreaks. Consequently, there is a need for a better quantitative understanding of the causalities and cross-scale interactions leading to large-scale outbreaks (Raffa et al., 2008; Seidl et al., 2016b; Senf et al., 2017). Typically, the growth of pest populations is described at the stand-level, using population models or system dynamics (Ludwig et al., 1978; Clark et al., 1979; Fernández and Fort, 2009; Lewis et al., 2010; Fahse and Heurich, 2011). This, however, does not reveal how local phenomena translate into large-scale dynamics. Although there are models describing spatial dynamics (Zhou and Liebhold, 1995; Logan et al., 1998), a multi-scale perspective on pest outbreaks has mainly been presented through a phenomenological (Peters et al., 2004; Raffa et al., 2008) or an empirical lens (Bjørnstad et al., 2002; Seidl et al., 2016b; Senf et al., 2017) to date. For successful pest management an integrated quantitative perspective on pest outbreaks is needed, which describes the propagation of pests as a function of landscape topology and host-pest interactions. Such a perspective - translated into a formal mathematical model of multi-scale outbreak dynamics - can lead to improved outbreak prediction and the design of effective anticipatory actions to mitigate outbreak losses. To achieve this perspective, we harness the increased availability of high-resolution spatial data on pest outbreaks and link ecological insights with multi-scale network theory (Strogatz, 2001; Urban and Keitt, 2001).

Networks have first been introduced in ecological studies through

* Corresponding author.
E-mail addresses: wildemee@iiasa.ac.at (M. Wildemeersch), franklin@iiasa.ac.at (O. Franklin), rupert.seidl@boku.ac.at (R. Seidl), rogelj@iiasa.ac.at (J. Rogelj), moorthy@iiasa.ac.at (I. Moorthy), stefan.thurner@meduniwien.ac.at (S. Thurner).

https://doi.org/10.1016/j.ecolmodel.2019.108745
Received 12 March 2019; Received in revised form 4 July 2019; Accepted 9 July 2019

the use of economic input-output models to analyze structural properties of ecosystems and their impacts on synergism and stability (Hannon, 1973; Finn, 1976; Patten, 1978; Ulanowicz, 1980; Fath and Patten, 1999). In the field of epidemiology, compartmental models initially looked at disease spread in a fully mixed population, meaning that an infected individual is equally likely to spread the disease to any other member of the population (Kermack and McKendrick, 1991). Due to the wide occurrence of complex networks in nature, network based approaches developed for modelling the spread of epidemics have later also been considered to study the spread of computer viruses (Pastor-Satorras and Vespignani, 2001), the spread of sexually transmitted diseases (Newman, 2002), for approximation techniques (Keeling and Eames, 2005), and the development of strategies to counter virus spread in real networks (Chakrabarti et al., 2008). Until 2010 almost all network research focused on the properties of a single network, but since most natural systems are composed of multiple subsystems, interconnected networks have received increasing attention in order to improve the understanding of real complex networks (Gao et al., 2012a, 2014). In ecology, networks of networks (NoNs) have been used to study the spread of invasive species through the combination of social and ecological networks (Haak et al., 2017), and networks of species interactions have been studied in view of species decline and extinction (Pocock et al., 2012). Many interconnected networks also account for spatial constraints. The main advantage of these so-called embedded networks over other spatially explicit models is that spatially-explicit phenomena can occur at different scales. As an example in epidemiology, multi-scale mobility processes based on gravity models have been analyzed and the effects on disease spread of short-range commuting versus long-range airline traffic have been evaluated (Balcan et al., 2009).

Here, we present a general framework to determine the spread of a pest over a landscape accounting for large-scale factors related to the landscape topology, as well as small-scale factors that result from varying pest pressure. First, we present the building blocks of the framework. Subsequently, we illustrate the effectiveness of the approach in capturing the pest dynamics of two fundamentally different pest species. Finally, we illustrate how the framework can be used to guide landscape-scale pest management. Building on network concepts (Strogatz, 2001; Messier et al., 2013) we demonstrate how anticipatory forest management, catered to the landscape rather than the individual stand, can optimize pest control (Seidl et al., 2018).

2. Material and methods

2.1. A multi-scale analysis of pest spreading

We apply a multi-scale network approach, and develop a network of networks comprising a large-scale and a small-scale network. The large-scale network considers the landscape as a network of habitat patches, while the small-scale network examines individual habitat patches (Fig. 1a). The nodes in the large-scale network represent habitat patches, whereas nodes in the small-scale network represent grid cells within a patch. Temporal variability (e.g., pest pressure) is captured by the small-scale network, while spatial connectivity (i.e., contagion/dispersal) is captured by the large-scale network. Weather effects, such as precipitation and temperature, influence pest development and spread within a patch, while the distance between habitat patches affects the possible spread of a pest between patches throughout the landscape.

The modular framework presented here consists of a landscape module, which captures the pest propagation over the large-scale network, and a stand module, which captures the percolation of the pest through a small-scale habitat patch. The framework is constructed according to the following three steps (Fig. 1b): On the landscape scale, we first identify the potential habitat patches of the pest and determine the connectivity between habitat patches based on the dispersal capability of the species under consideration. The outcome of this step is a network of habitat patches. Next, we formulate how a pest spreads over the constructed network. The study of disease propagation has evolved from unstructured populations to networked populations, using a variety of epidemic models (Newman, 2002; Pastor-Satorras and Vespignani, 2002). Depending on the specific pest under consideration, we select the appropriate epidemic model to describe the network dynamics. We can, for instance, differentiate between cases where the passage of the pest is followed by host-recovery (Appendix A) or host-mortality (Appendix B). We here propose a probabilistic model that evaluates over time the probability of each node in the large-scale network to be in a given state, i.e. susceptible (S), infested (I), or removed (R). Although the epidemic model operates at the landscape scale, the model reacts to changes occurring in the small-scale networks. In the last step, we define the temporal variation in the pest pressure, active at the local scale, through a suitable model of the host-pest interactions (Appendix C), which represents the time-varying probability that a pest percolates through a local habitat patch (Appendix D). The number of model parameters required by our framework is small. At the local scale, β_S indicates the probability that an infestation disperses through a patch, while at the landscape scale, β_L specifies the probability that a pest spreads to a neighbouring node, the recovery rate δ represents the probability that an infested node recovers in a single time step, and γ is the probability that an infested node dies. The connectivity of the large-scale network is fully determined by adjacency matrix A and the spectral radius $\lambda_1(A)$ of the adjacency matrix, which is the dominant eigenvalue of A indicating whether the presence of a pest species will lead to an outbreak or not. The combination of the network structure, the large-scale spreading, and the small-scale variations in the pest pressure, makes it possible to describe the evolution of the fraction of susceptible habitat patches, infested habitat patches, and dead habitat patches, where applicable.

2.2. Geometrid moth outbreaks in birch forests

In a first case study we consider the outbreak dynamics of geometrid moths (*Epirrita autumnata* and *Operophtera brumata*) in boreal birch forest of Fennoscandia, covering the northern parts of Norway, Sweden, and Finland (Jepsen et al., 2009b). We construct the network by using a spatio-temporal dataset over the years 2002 to 2010. The dataset originates from satellite imagery and consists of annual binary defoliation maps with a spatial resolution of 250 m × 250 m. Defoliation scores were previously shown to be an appropriate proxy for larval densities measured on the ground (Jepsen et al., 2009a). Using the forest mask of the area and based on geographical separation, the area is divided into habitat patches that correspond to nodes in a large-scale network (Fig. 2a). Subsequently, network connectivity is determined by comparing the minimum distance between patches with the dispersal capability of the species, i.e., the maximum distance that moths can cover to find new hosts or mates. Based on expert knowledge, we use a baseline dispersal distance of 1500m. Merging the node and link data, a landscape network is obtained (Fig. 2b) (Urban and Keitt, 2001). A network node in the large-scale network is considered infested if the fraction of infested grid cells within a forest stand exceeds a specified threshold η (Fig. 2d). We observe that the appearance of outbreaks can consistently be detected under a wide range of threshold values (Fig. 2d). The value $\eta = 0.5$ is selected as the minimum value that discerns three defoliation episodes originating from local outbreaks occurring in different habitat patches, as can be observed from our example dataset.

We adopt the SIS (susceptible-infested-susceptible) epidemic model (Chakrabarti et al., 2008) and account for multiple scales by linking the small-scale and large-scale factors in the model. The large-scale epidemic model hinges upon the infestation rate $\beta = \beta_L\beta_S$,

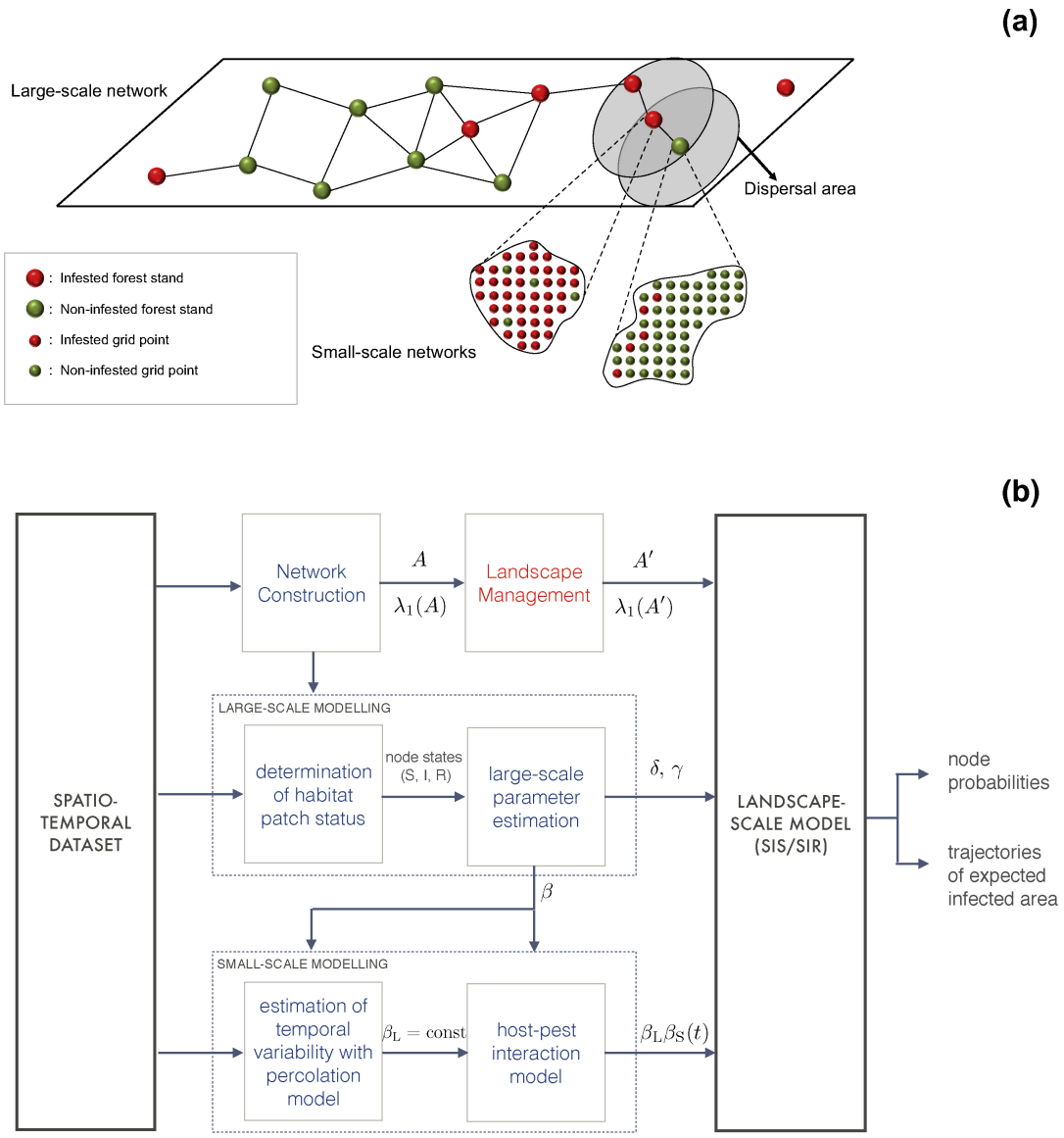

Fig. 1. Conceptual view on multi-scale pest outbreaks. (**a**) A network of networks to describe interacting spatial scales. The shaded area in the large-scale network represents the dispersal range over which the eruptive pest can spread. When a patch falls within the dispersal range of another patch, the network nodes are connected. Here we consider Euclidean distance, but the metric can be extended to any other effective distance that accounts for dispersal barriers in the landscape such as mountains. In the small-scale network, grid cells constitute a lattice network where each cell is connected to its direct neighbours. (**b**) Building blocks of the multi-scale modelling framework. The spatio-temporal dataset is used for network construction and the estimation of the large-scale and small-scale parameters. The adjancency matrix A, infestation rates β_L and β_S, the recovery rate δ, and the removal rate γ are used in the landscape-scale model to monitor infested area, estimate risk, and evaluate the effectiveness of landscape-scale forest management.

which represents the product of large-scale and small-scale infestation rates, and the recovery rate δ. The succession of outbreak and recovery phases indicate that β varies over time. The variation in β is due to the small-scale factor β_S, as will be shown later, and is modeled by means of a predator-prey model. The infestation probabilities β_S and β_L are active at different time scales, and we assume that β_L is time-independent. A detailed mathematical description of the network dynamics, both large-scale and small-scale, is provided in Appendices A and C. The appendices also contain the parameter values used to validate the model.

2.3. European spruce bark beetle outbreaks in a temporate forest

In a second case study, we consider the outbreak dynamics of the European spruce bark beetle (*Ips typographus*), based on a time series of outbreak dynamics from 1990 to 2012 in the Bavarian Forest National Park (Seidl et al., 2016b). The data set contains the binary infestation status over the considered period with a spatial resolution of 30 × 30m over a total area of 13 319 ha, and covers two distinct epidemics over this period. The network structure is derived from the definition of the habitat patches based on geographical separation (Fig. 3a) and a maximum dispersal capacity of 253 m (Seidl et al., 2016b). The resulting network structure is shown in Fig. 3b. The main phenomenological difference with respect to geometrid moths is that trees die after bark beetle infestation. The state of habitat patches can therefore be categorized as susceptible (S), infested (I), and removed (R). In order to classify the habitat patches into these three states, two thresholds η_I and η_R are introduced that compare the fraction of infested and

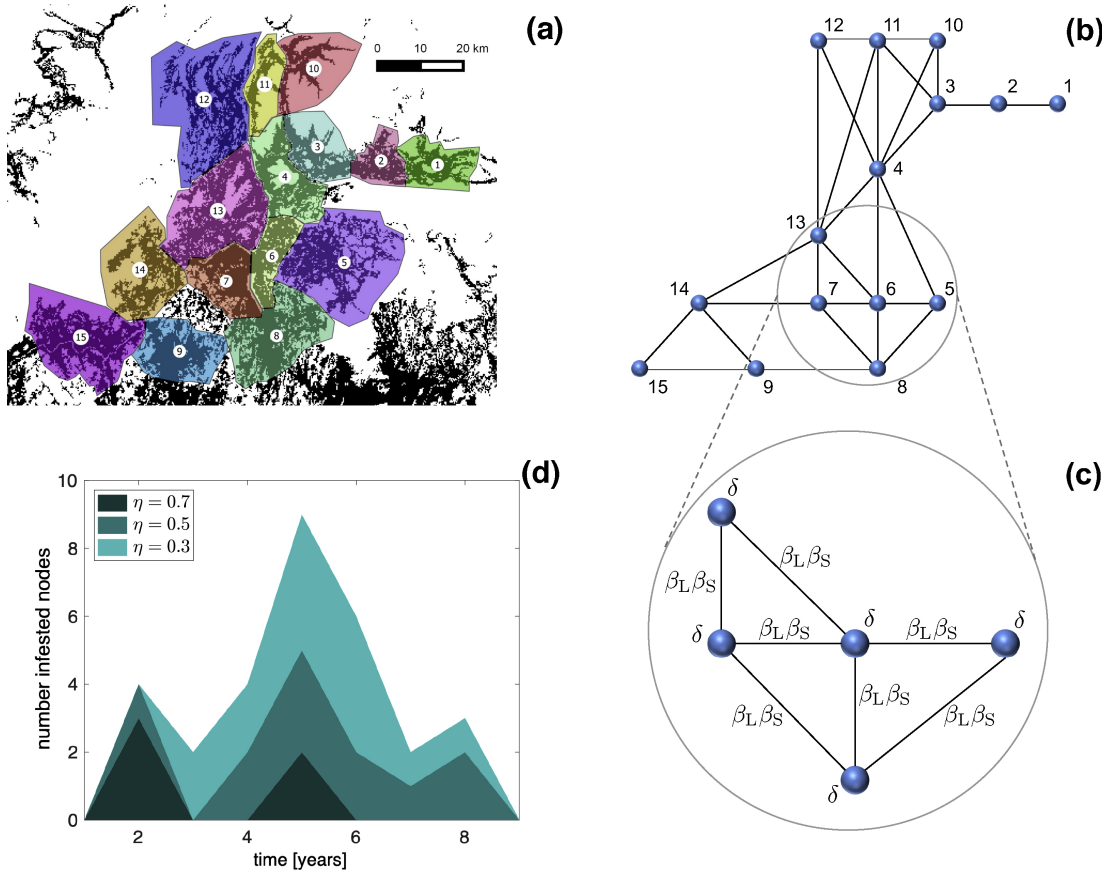

Fig. 2. Network construction for geometrid moth case study. (**a**) Definition of habitat patches for an illustrative study region in Fennoscandia. (**b**) Network representation of the landscape under consideration. (**c**) The spreading of a pest over the network is represented by an SIS (susceptible-infested-susceptible) model with homogeneous infestation rate $\beta_L\beta_S$ and recovery rate δ. (**d**) Comparison of the fraction of infested grid cells within a patch with different threshold values η to determine the state of network nodes.

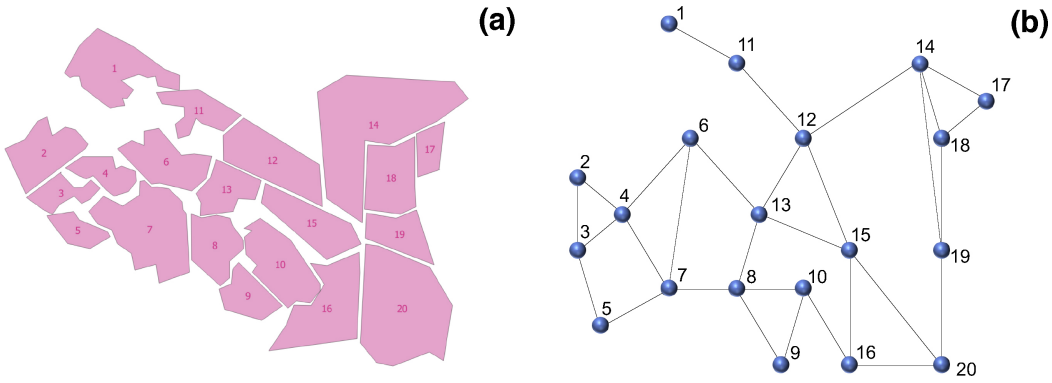

Fig. 3. Network construction for bark beetle case study. (**a**) Habitat patches of the spruce bark beetle in the Bavarian Forest National Park. (**b**) Network representation of the habitat patches and their connectivity.

removed cells within a habitat patch to their corresponding threshold. A habitat patch is infested if the fraction of infested grid cells within the habitat patch is greater than η_I, and the habitat patch is removed if the fraction of removed grid cells within the patch is greater than η_R. The values of the thresholds are set to $\eta_I = 0.07$ and $\eta_R = 0.6$, determined by matching the shape of the infestation probability of cells in the entire data set to the infestation probability of nodes in the network to find η_I, and using an analogous approach to find η_R.

At the landscape scale, we adopt an adjusted SIR model with possible transitions between the susceptible and infested states indicated by the infestation rate β, between the infested and susceptible states represented by the recovery rate δ, and between the infested and removed states described by the removal rate γ. Similar to the moth case study, the bark beetle data set contains a succession of epidemic and recovery phases, which indicates that the infestation rate is time-dependent. The evolution of β is modeled by means of a predator-prey

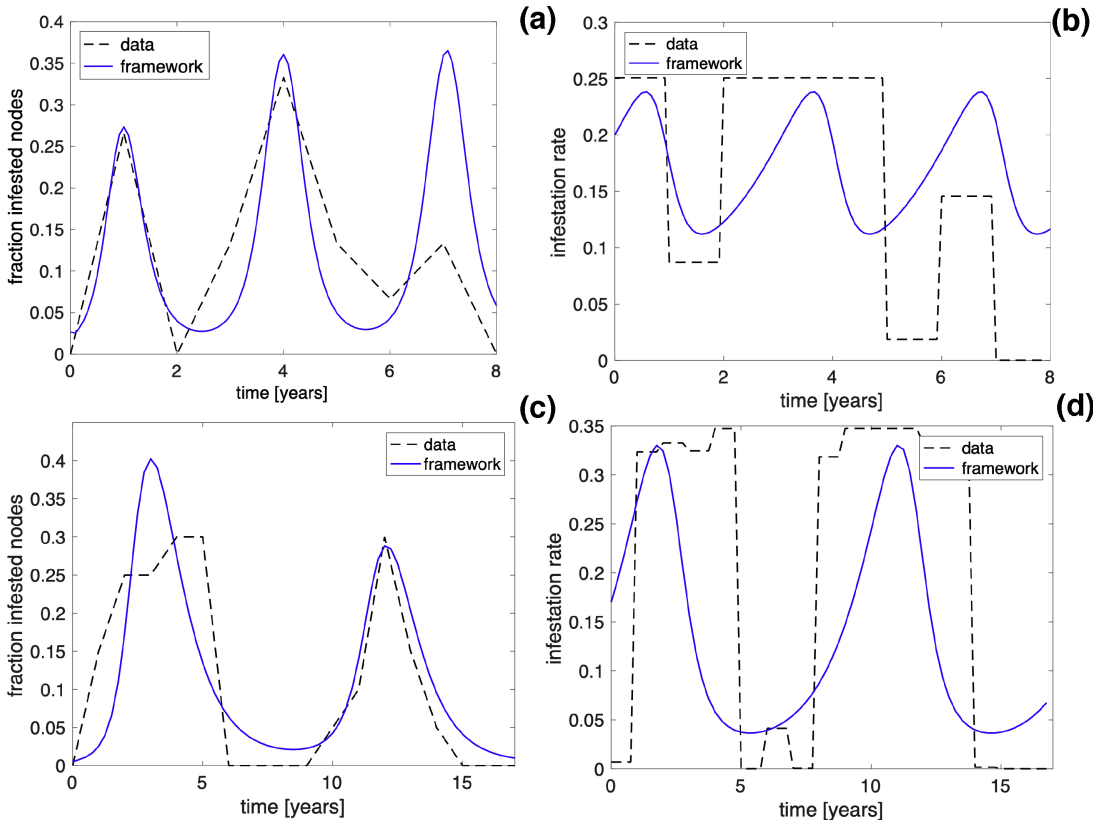

Fig. 4. Model validation for the geometrid moth (top) and spruce bark beetle (bottom). (**a**) Validation of the framework by comparing the fraction of infested nodes over time predicted by the analytical framework to observed data. (**b**) Comparison between time-varying pest pressure as from the modelling framework and the evolution of the observed percolation probability. (**c**) Validation of the framework for the spruce bark beetle case study: A comparison of infestation probability over time predicted by the modelling framework versus observed data. (**d**) Comparison between the development of the pest pressure and percolation probability, indicating that the varying infestation probability originates from small-scale factors.

model. A detailed mathematical description of the building blocks of the model can be found in Appendix B and Appendix C, as well as the parameter values used to validate the model.

2.4. Early warning and risk monitoring

Building on this modular framework, we define first an epidemic threshold that determines whether the ecosystem is in the epidemic or non-epidemic regime (see Appendix E and F). Then, we use the distance to the epidemic threshold as a risk measure for pest outbreaks, so that the framework allows us to track outbreak risk over time.

The presented modelling framework enables us to discriminate between two regimes that are typical for pest outbreaks, i.e., epidemic and non-epidemic conditions. Additionally, the model relates the dynamics of the system and its switching between these two regimes to small-scale and large-scale drivers by means of a parsimonious set of parameters. This limited set of system parameters, which can be directly estimated from spatial data and observations, allows us to define the threshold for the transition between non-epidemic and epidemic conditions. Whether or not analytically tractable solutions can be found, depends on the formulation of the model. If no analytical solution is possible, regions of epidemic and non-epidemic conditions can always be determined by simulating a particular instance of the model. Here, we use the geometrid moth case study, which has tractable solutions, to demonstrate how the framework can be used to inform landscape-scale pest management. For the large-scale model with SIS dynamics, it can be shown (see Appendix E) that the ecosystem is in the non-epidemic regime with decreasing infestation probability when the following condition is met

$$\frac{\beta_L \beta_S}{\delta} < \frac{1}{\lambda_1(A)}, \tag{1}$$

which means that the ratio of infestation rate β to recovery rate δ is smaller than a certain value determined by the landscape topology (defined by $1/\lambda(A)$). Conversely, the system is in the epidemic regime when $\beta_L \beta_S/\delta > 1/\lambda_1(A)$. This result reveals that small-scale and large-scale factors interact in a multiplicative way in regime shifts from non-epidemic to epidemic behavior. Small-scale factors exhibit rapid changes over time as will be demonstrated later, and pest outbreaks are very sensitive to these changes on the local scale such that small changes in pest pressure can have substantial effects on the landscape-scale behavior. Eq. (1) also reflects the relevance of the network structure through the spectral radius of the adjacency matrix. Probabilistic insights can be obtained for landscape topologies with similar spatial characteristics in terms of forest density. We can determine a lower bound of the epidemic threshold for a landscape characterized by a forest density μ and a dispersal capability R, which is given by (see Appendix F)

$$\frac{\beta_L \beta_S}{\delta} < \frac{1}{l\mu R^2} < \frac{1}{\lambda_1(A)}, \tag{2}$$

with l a constant defined in the Appendix F. Eq. (2) provides general insight how the interaction between pest dispersal capability and forest density affects the epidemic threshold. Specifically, the lower bound of the epidemic threshold is inversely proportional to the forest density and the square of the dispersal capability. This result shows the sensitivity of outbreak dynamics with respect to the dispersal capability.

It is notably hard to predict critical transitions (Scheffer et al., 2009;

Carpenter, 2013; Dai et al., 2013). Similar to early-warning signals based on the statistical analysis of past system behavior (Scheffer et al., 2009), the proposed analytical framework requires sufficient historical data, in this case to estimate the model parameters. However, in contrast to statistical indicators of regime shifts, our analytical framework provides parameter space trajectories that allow us to track the risk of pest outbreaks over time, as a function of key ecological parameters. The distance in parameter space to the critical threshold gives indications about the likelihood of an outbreak, which enables an anticipatory approach in ecosystem management, responding to risk rather than to incidence of events (Seidl, 2014). The distance to the epidemic threshold provides a quantification of the risk of regime shifts between epidemic and non-epidemic conditions based on the system parameters β_L, β_S, δ, and $\lambda_1(A)$.

3. Results

3.1. Multi-scale model provides outbreak dynamics consistent with data

The modelling framework can simultaneously simulate population dynamics at the small scale and spreading behavior at the large scale. In the case study of the geometrid moths, a single population features decadal cycles, but by aggregation of data over the considered area we observe three defoliation episodes with a periodicity of three years (Fig. 4a). The three year periodicity originates from different outbreak episodes occurring in different habitat patches, which is taking place due to network effects. Note that in the presented test case we capture the aggregate pest pressure originating from two moth species that feed on a common host, while underlying processes and factors (e.g., species differences) that generate the aggregate pest pressure are implicit. The effectiveness of the framework in capturing the moth outbreak dynamics is illustrated by analyzing the fraction of infested area over time (Fig. 4a), showing good agreement between model and data and a coefficient of determination of $R^2 = 0.6$. The modelling framework is able to reproduce the epidemic and non-epidemic phases with accurate frequency, and the magnitude of the outbreaks can be reproduced well for the first two outbreaks. The smaller magnitude of the third peak cannot be reproduced by the analytical tool due to the deterministic evolution of β. Higher temporal resolutions of the available data and an adaptive algorithm to adjust the parameters of the predator-prey model over time could resolve this issue in future work.

The predator-prey dynamics are much faster than the temporal variation in large-scale factors affecting spreading probability, which leads to the assumption of time-varying small-scale factors captured by β_S and time-invariant large-scale factors captured by β_L. We test this assumption by estimating the probability that an infestation percolates through the small-scale habitat patch based on observations (A detailed mathematical description can be found in Appendix D) and comparing this with the time-varying pest-pressure in the model. Comparing the percolation probability arising at the small-scale with the modeled trajectory for β (Fig. 4b), we observe a good match indicating that the large-scale pest dynamics emerge from variations in the small-scale factors, and justifying the assumption of time-invariant large-scale factors.

For the case study of the spruce bark beetle, the model is also deployed to monitor the state of the network nodes over time. Focusing on the infested network nodes, we find good agreement between the fraction of infested area derived by the model versus the observed data, with a coefficient of determination of $R^2 = 0.67$ (Fig. 4c). We also verify that the dynamics of the infestation rate β stem from the local-scale factors by estimating the percolation probability and comparing it with the evolution of β (Fig. 4d). As in the moth case study, we find that the observations are consistent with time-independent large-scale factors and time-dependent small-scale factors.

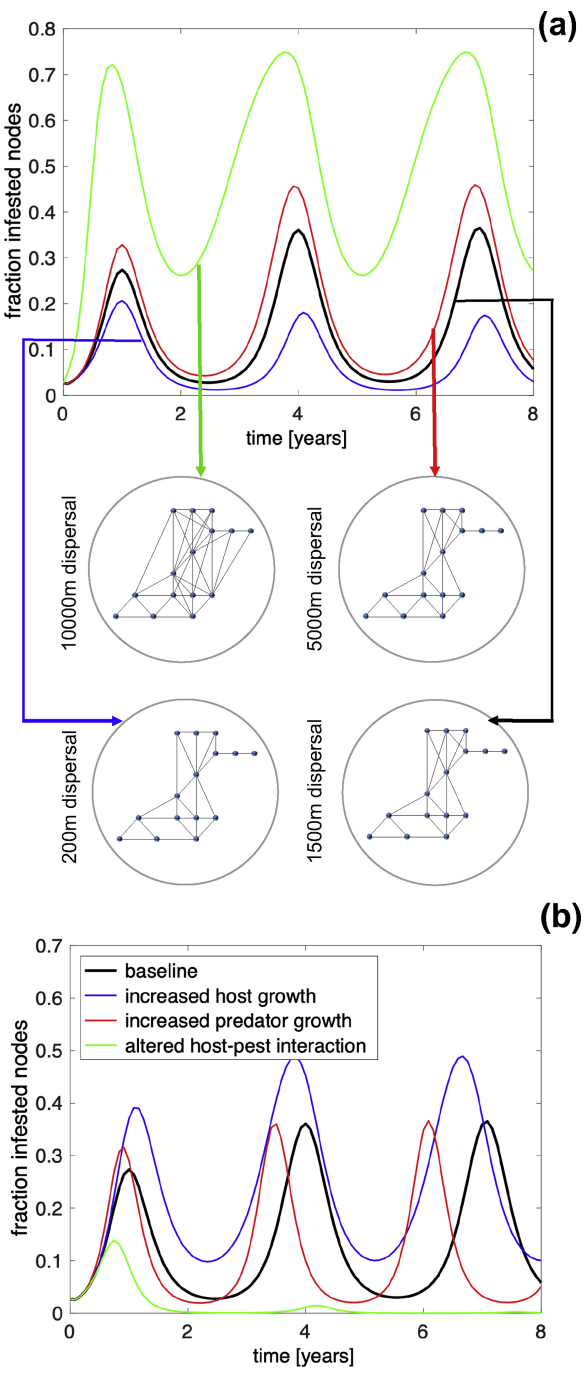

Fig. 5. Sensitivity analysis of the pest outbreak framework. (**a**) Sensitivity analysis with respect to large-scale factors. The modification of network connectivity is driven by variation in dispersal capability and results in a change of the adjacency matrix A' as depicted in Fig.1b. (**b**) Sensitivity analysis with respect to small-scale factors. The alteration of the host-pest interactions is driven by the variation of the four parameters of the predator-prey model as described in Eq. (C.1) of Appendix C. The relative change of the parameter affecting host growth was 12%, the parameter affecting predator growth 50%, and the parameters affecting the host-pest interaction 15% (see Appendix G).

3.2. Pest outbreaks are driven by pest pressure fluctuations at the local scale modulated by the landscape structure

As a result of its modular structure, the sensitivity of the model can be analysed separately for large-scale and small-scale factors (Fig. 5a and b). We here use the geometrid moth case study to illustrate the

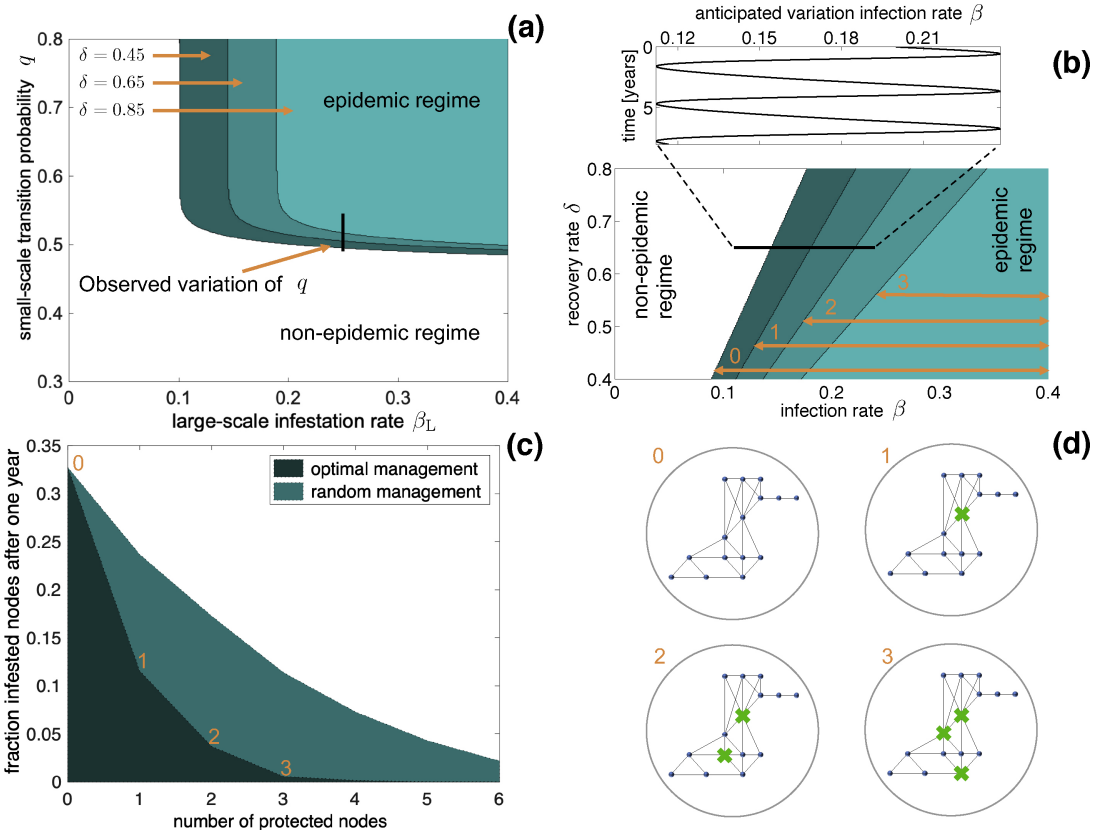

Fig. 6. Quantitative support for optimal landscape-level management of pest outbreaks. (**a**) Epidemic region in the parameter space of β_L and q, for the network indicated by 0 in **d**. (**b**) Epidemic region in the parameter space drawn by β and δ. We observe how the epidemic region decreases with successive management of stands, in order to decrease connectivity as indicated in **d**. (**a-b**) The ecosystem trajectory through the epidemic and non-epidemic regions is indicated by the black line for $\beta_L = 0.25$ in **a** and $\delta = 0.65$ in **b**. (**c**) Comparison of optimal and random management strategies with parameter values $\beta = 0.21$ and $\delta = 0.65$, corresponding to the parameters of the second outbreak wave in Fig. 2e. By exploiting the knowledge of the network structure, the optimal management strategy leads to a substantial reduction of the infested nodes after one year. (**d**) Illustration of the successive steps in the optimal management of the landscape. The spectral radii are given by $\lambda_1(A) = 4.53$ for network 0, $\lambda_1(A) = 3.61$ for network 1, $\lambda_1(A) = 2.98$ for network 2, and $\lambda_1(A) = 2.33$ for network 3.

sensitivity of the model to factors manifesting at different scales. With regard to large-scale factors, we alter the network connectivity by assuming different dispersal capabilities (Fig. 5a). We observe that modest changes in network connectivity can lead to substantial changes in the magnitude of outbreaks. With regard to small-scale factors, we evaluate how changes in the host-pest interaction affect the number of infested nodes over time. We observe that the variation of the trajectories of the infestation rate β (see Appendix G, Fig. G.8) results in radically different outbreak behaviour, both in terms of outbreak frequency and magnitude. Using modifications in the network connectivity and the host-pest interactions, the sensitivity analysis demonstrates that outbreak dynamics are responsive to small changes in both large-scale and small-scale parameters. This supports the hypothesis that pest outbreak behaviour can only be captured correctly through an accurate understanding of the cross-scale interactions of landscape topology and host-pest dynamics.

3.3. Selective landscape management necessary for efficient outbreak prevention

Based on the epidemic threshold, we can distinguish between epidemic and non-epidemic regimes, and moreover, the distance to the epidemic threshold provides a quantification of the risk of regime shifts between epidemic and non-epidemic conditions. As an example, the epidemic region depicted in the space defined by the large-scale infestation rate β_L and the transition probability q (indicating the measurable probability that an infested cell contaminates neighbouring cells) illustrates the high sensitivity of the system dynamics to small-scale factors, since small variations of the transition probability q can result in a regime shift (Fig. 6a). In addition, we observe how the size of the epidemic region decreases with increasing recovery rate δ. It is also possible to reduce the outbreak risk, in terms of the size of the epidemic region in the parameter space, through the removal of infested cells or the introduction of dispersal barriers (Fig. 6b). In this case, the decrease of the epidemic region results from a decrease of the spectral radius due to the changing network structure as a result of the management actions. The decrease of the spectral radius corresponds to an increase of the epidemic threshold, as can be deduced from Eq. (1). The trajectory of the ecosystem through the epidemic and non-epidemic regions provides us with a quantification of how outbreak risk evolves over time (Fig. 6a and b). In fact, the trajectory in parameter space provides early warning signals and can be used to evaluate the effectiveness of potential management strategies. For instance, we observe that through targeted management of three forest stands, the ecosystem trajectory remains completely in the non-epidemic region of the parameter space in the geometrid moth example (Fig. 6b). Importantly, rather than being solely determined by historical pest observations, our early warning signals encapsulate mechanistic knowledge of the ecosystem and the environmental drivers in addition to the observations.

Since the epidemic threshold is inversely proportional to the spectral radius, the optimal management strategy exploits the knowledge of the network structure by protecting the node in the network that has

the largest effect on the spectral radius. Such a targeted management strategy results in a maximal increase of the non-epidemic region in parameter space (Fig. 6b). In order to benchmark pest management strategies, the mathematically optimal strategy can be contrasted with random actions (Fig. 6c), and the benefit of targeted management quantified in terms of the gain in healthy forest area. The model-determined optimal strategy consistently results in large gains of forest area not infested by the pest relative to the random-protection strategy.

4. Discussion

Empirical evidence has shown that outbreak dynamics of pests are driven by multi-scale processes (Senf et al., 2017; Seidl et al., 2016b; Raffa et al., 2008). Through a phenomenological analysis, multi-scale drivers were identified (Raffa et al., 2008), and the relative importance of different drivers was determined by means of statistical analysis (Senf et al., 2017). This study provides a first analytical model for pest outbreaks that incorporates multi-scale drivers and their interactions. We have shown that the model is capable to reproduce the outbreak dynamics of forest insects that feature very different epidemic behavior. The analytical modelling framework provides opportunities to include multi-scale perspectives into management practices.

The modelling framework presented here has been designed for parsimony, based on a basic model for predator-prey dynamics and an epidemic model with parameters that are homogeneous over space. Nevertheless, homogeneous interactions between network nodes are sufficient to yield good agreement between model results and the available data. The flexibility of the framework allows us to incorporate different building blocks in order to adapt it to different types of epidemic behavior and/or host-pest interactions. The building blocks of our model can easily be replaced by more advanced ones in the future, for example including pest antagonists or introducing spatially variable infestation rates. With respect to the structure of the network of networks, the small-scale lattice network is directly driven by the resolution of the available satellite imagery, while the large-scale network identification could be improved by designing a classification algorithm. In order to make the framework applicable for actual forest management, other aspects such as administrative boundaries and specific habitat characteristics could also be included. Although climate-dependent and climate-independent factors have been identified in our framework, climate effects are currently only implicitly included in the model (see Appendix G, Table G.1). Addressing the relationship between climate effects and outbreak occurrence more explicitly in future work could allow us to assess the robustness of pest management strategies under changing climate conditions. Further limitations of our current framework are that variable development trajectories of hosts, and subsequently their susceptibility, are not considered (Seidl et al., 2016a). The framework can represent dispersal of a species up to the landscape scale, and in order to expand the model to the regional scale other effects should be included such as long-range infestations (Cain et al., 2000; Mundt et al., 2009).

In spite of these limitations, the case studies involving two strongly differing pest species (defoliator, bark beetle) indicate that the presented framework is sufficiently flexible to capture the relevant phenomena governing pest outbreak waves in ecosystems. The modelling framework is generally applicable to a wide range of systems due to its modular setup, with practical relevance as a toolbox for early warning and landscape-level disturbance management. By integrating different sources of complex dynamics, an effective model for pest outbreaks has been developed that quantifies the relevance and relation between small-scale and large-scale factors. The sensitivity analysis underlines that both the host-pest interactions at the local scale and the network structure at the landscape scale drive pest dynamics in forest ecosystems. Consequently, the inclusion of spatially explicit landscape-scale data as well as host-pest interactions is crucial for an accurate quantification of outbreak dynamics, yet remains neglected in many pest models (e.g. Dietze and Matthes (2014)).

Forest managers currently tackle biotic disturbances mostly at the patch level, and largely neglect the relevance of landscape effects (Seidl et al., 2016b). However, the speed at which pests spread through fragmented habitats is largely governed by the network connectivity (Margosian et al., 2009; Meentemeyer et al., 2012). The danger of over-connected systems (Fig. 5a) calls for a multi-scale perspective in outbreak management, and the proposed framework fosters such a perspective by consistently integrating drivers at different scales (Cornelius et al., 2013). This is in line with previous research indicating an increased vulnerability of networks of networks compared to single networks (Gao et al., 2012b). Several silvicultural practices such as sanitation felling and introducing dispersal barriers can efficiently be tested as virtual immunization strategies (Long, 2009) with our framework, in order to improve future pest management.

5. Conclusions

From an applied science perspective, the most important implication of this work is that our quantitative model of pest dynamics can be used in landscape-scale forest management. The modelling framework provides outbreak trajectories that allow an assessment of future areas at risk of disturbances. Exploiting the knowledge of landscape topology, a targeted management strategy that optimally mitigates the spreading potential of a pest can be devised a priori. Whereas reducing habitat quantity has been discussed in the past (Senf et al., 2017), our model identifies which habitat patches contribute most to the risk of pest spreading, which in turn allows us to develop an optimal landscape-scale management scheme. Our results show that the optimal management scheme yields gains of uninfested forest area up to 15% with respect to random habitat reduction in the example of geometrid moth outbreaks. These capabilities are especially timely and important given the growing concern about changing disturbance regimes (Seidl et al., 2017).

Authors' contributions

MW led the overall research project, developed and implemented the multi-scale model, and led the writing of the paper. MW, OF, and ST were involved in designing the research. OF, RS, JR and ST contributed to writing the paper. IM assisted in handling the GIS data.

Data availability

The data used in the bark beetle case study are archived in the Dryad Digital Repository doi: 10.5061/dryad.c5g9s. Additional data related to this paper may be requested from the authors.

Acknowledgements

The authors acknowledge Jane Uhd Jepsen for providing access to the dataset of geometrid moth outbreaks in Fennoscandia and for critically reviewing the paper. RS acknowledges support from the Austrian Science Fund through START grant Y895-B25, as well as through the EU ERA-Net Sumforest project REFORCE (BMLFUW Austria grant 101198).

Appendix A. Large-scale, landscape module with SIS dynamics

When the SIS model is used to describe the large-scale dynamics, the network nodes can be in the susceptible or infested state. The SIS model we use here is defined by the infestation rate β, which indicates the probability that an infested node infects a neighbouring node in one time step, and a constant recovery rate δ, which represents the probability that an infested node heals in a single time step. The infestation rate $\beta = \beta_L \beta_S$ consists of the large-scale rate β_L, which specifies the probability that a pest spreads to a neighbouring patch, and the small-scale rate β_S, which indicates the probability that an infestation percolates through a patch. By assuming that the spread at the landscape scale can only proceed once an outbreak occurred on the local scale, we make the connection between small-scale and large-scale factors explicit, and consider cross-scale amplifying interactions (Peters et al., 2004; Seidl et al., 2016a). The network structure is uniquely defined by the adjacency matrix A, and the parameters β_L and β_S are assumed homogeneous in space and equal to the expected value of the infestation rates. The dynamics of the infestation across the network are represented by a system of difference equations with state vector $\mathbf{p}(t) = (p_1(t), \ldots, p_n(t))$, containing for each node the infestation probability that changes over time according to a stochastic process. We settle on a discrete time dynamic model to express the evolution of $\mathbf{p}(t)$ (Chakrabarti et al., 2008). Let $\zeta_i(t)$ denote the probability that node i does not get infested at time t, which can be written as

$$\begin{aligned}\zeta_i(t) &= \prod_{j \in \mathcal{N}_i} [p_j(t-1)(1-\beta_L\beta_S) + (1-p_j(t-1))] \\ &= \prod_{j \in \mathcal{N}_i} (1 - A_{ij}\beta_L\beta_S p_j(t-1)),\end{aligned} \tag{3}$$

where A_{ij} are the entries of the adjacency matrix and $\mathcal{N}_i$ stands for the neighbourhood of node i, i.e., the nodes j that are connected to node i. The dynamics of the infestation probabilities over the network can be written as the vector function $p_i(t) = f_i(\mathbf{p}(t-1), A, \beta, \delta)$, where $f_i(\mathbf{p}(t-1), A, \beta, \delta)$ is defined as

$$f_i(\mathbf{p}(t-1), A, \beta, \delta) = 1 - (1 - p_i(t-1))\zeta_i(t) - p_i(t-1)\delta\zeta_i(t) \tag{4}$$

$$= 1 - \prod_j (1 - A_{ij}\beta_L\beta_S p_j(t-1))[1 + (\delta - 1)p_i(t-1)]. \tag{5}$$

The second term in (4) represents the probability that a healthy node does not get infested, and the third term designates the probability that an infested node heals in the considered time step. The function f_i is a non-linear function of the infestation probabilities, and reflects the role of large-scale factors, small-scale factors, and landscape topology through β_L, β_S, and A. The parameters β and δ are estimated in the least squares sense using the observed trajectory of the number of infested nodes. The value of the constant recovery rate is $\delta = 0.65$, and the time-dependent value of β minimizing the modelling error is passed to the small-scale stand module.

Appendix B. Large-scale, landscape module with SIR dynamics

When trees or crops do not recover from infestations, they can be in the susceptible, infested, and removed state. Under these conditions the dynamics are described by the so-called SIR model (Draief et al., 2008). In the case of bark beetles, trees get infested by beetles dispersing from infested neighbors, and can transmit the infestation further once the next generation of beetles disperses. On an individual level, the traditional SIR model with transitions from the susceptible to the infested state, and from the infested to the removed state is suitable. Nonetheless, by aggregating data over a habitat patch, we observe that the transition from the infested state to the susceptible state is also possible. This happens when the fraction of infested nodes is too low to pass the threshold for the node to become removed. The SIR model presented in this section is therefore a combination of the traditional SIS and SIR models. Once a network node is removed, it cannot become infested or susceptible again. In the adjusted SIR model, the dynamics of the infestation over the network are captured by the adjacency matrix A, the infestation rates on the small scale and landscape scale β_S and β_L, the recovery rate δ, and the removal rate γ. Since nodes can be in three different states, the dynamics can be described by two sets of difference equations, and the probability of the third state can be obtained as the complement of the two other states. Similar as for the SIS model, we define the probability that node i does not get infested at time t as

$$\begin{aligned}\zeta_i(t) &= \prod_{j \in \mathcal{N}_i} [(p_j^S(t-1) + p_j^R(t-1)) + p_j^I(t-1)(1-\beta_L\beta_S)] \\ &= \prod_j (1 - A_{ij}\beta_L\beta_S p_j^I(t-1)),\end{aligned} \tag{6}$$

where p_j^S, p_j^I, and p_j^R represent the probabilities that node j is in the susceptible, infested, and removed state, knowing that $p_j^S + p_j^I + p_j^R = 1$. The dynamics of the state probabilities can be written as three vector functions $\mathbf{p}^S(t) = f^S(\mathbf{p}^S(t-1), \mathbf{p}^I(t-1), A, \beta, \delta)$, $\mathbf{p}^I(t) = f^I(\mathbf{p}^S(t-1), \mathbf{p}^I(t-1), A, \beta, \delta, \gamma)$, and $\mathbf{p}^R(t) = f^R(\mathbf{p}^R(t-1), \mathbf{p}^I(t-1), A, \gamma)$. These vector functions can be expressed as

$$\mathbf{p}^S(t) = \mathbf{p}^S(t-1)) \odot \zeta(t) + \mathbf{p}^I(t-1)\delta \tag{7}$$

$$\mathbf{p}^I(t) = \mathbf{p}^S(t-1) \odot (1 - \zeta(t)) + (1 - \gamma - \delta)\mathbf{p}^I(t-1) \tag{8}$$

$$\mathbf{p}^R(t) = \mathbf{p}^R(t-1) + \gamma\ \mathbf{p}^I(t-1), \tag{9}$$

where $\odot$ stands for elementwise multiplication. Since the node probabilities sum to one, one of the difference equations can be omitted. Similar to the SIS model framework, we assume the parameters δ and γ to be constant, and β to be time-dependent, capturing the time-varying pest pressure. The values of β, δ, and γ are estimated in the least squares sense using the observed trajectory of the state of each network node. For the bark beetle case study presented here we find that the constant parameters take the values $\delta = 0.2$ and $\gamma = 0.05$, while the time-dependent value of β minimizing

modelling errors is passed to the small-scale stand module.

In both the SIS and SIR model, a mean field approach is applied by assuming homogeneous parameter values over the network for β, δ, and where applicable γ. For the SIS model, this assumption allows us to determine the critical threshold analytically. However, the mean field approach can be omitted and a numerical analysis for the spreading of infestation probabilities can also be performed for variable infestation and recovery rates. Although the results of the homogeneous model provide a good match with the available data, an inhomogeneous model can include more spatial precision.

Appendix C. Small-scale, stand module

It is essential that the framework captures the succession of outbreak and decay phases (Fig. 4a and c), which requires time-varying model parameters. As temporal outbreak patterns are strongly related to pest population pressure (Seidl et al., 2016b), we consider a time-varying small-scale infestation rate. This is motivated by the fact that the presence of more insects in one habitat patch will increase the probability of successful spreading to neighbouring patches. We model β as an endogenous variable in the analytical framework and model the time-varying $\beta(t) = \beta_L\beta_S(t)$ through host-pest interactions by means of a predator-prey model (Brauer and Castillo-Chavez, 2001). In our example, the prey is represented by the foliage or cambium pool of the forest, and the predator represents the pest population. Here, we use defoliation χ and infestation rate β as proxies for the prey and predator, respectively, and model the predator-prey dynamics of the network by means of the Lotka-Volterra equations

$$\begin{aligned} \frac{\partial \chi}{\partial t} &= a\chi - b\chi\beta \\ \frac{\partial \beta}{\partial t} &= c\beta + d\chi\beta\,. \end{aligned} \tag{10}$$

The parameterset $\{a, b, c, d\}$ determines the growth and decay of both predator and prey populations. For the estimation of the predator-prey model parameters, we have access to data relative to tree infestation, while data with respect to the predator stock is not available. We therefore generate the infestation rate that provides the best fit in the least-square sense between available data and analytical framework. The estimation of $\{a, b, c, d\}$ matches the parameters of (10) to the available data on infested trees and the estimated infestation rate determined in the large-scale landscape module. Since the outcome of the parameter estimation is sensitive to noise, the data is fitted to a three-term Fourier model before the estimation of the set $\{a, b, c, d\}$. In the geometrid moth case study we obtain the following parameter values $\{-0.81, -4.85, -0.04, -0.72\}$, while in the bark beetle case study we obtain $\{-0.8, -6, -0.7, -6\}$. The negative values of all parameters require more justification. Note that we use defoliation/tree infestation χ as a proxy for the prey. Since χ represents the complement of host foliage/bark, we require χ to decrease exponentially in the absence of the predator, and hence we find negative values for a. Since defoliation will increase with increasing populations of predator and prey, we also find a negative value for b. In the absence of prey, the predator population will extinguish and therefore we find negative values for c. Finally, predator abundance will decrease with higher defoliation, resulting in negative values for the parameter d. Through the predator-prey model, we capture the host-pest interaction, where the variation of β provides a density-dependent feedback to the epidemic model. In this respect, it is relevant to observe that the pest pressure is captured by means of an unstructured population, which is a mean field approximation for the entire region. The host-pest interaction model produces a trajectory of $\beta(t) = \beta_L\beta_S(t)$ with β_L considered time-invariant. This assumption is justified as the fluctuations in insect population are much faster than the dynamics of β_L (Fig. 4b and d). Note further that the population dynamics of the pest are strongly related to climate effects (see Appendix G, Table G.1) (Seidl et al., 2016b).

The model for host-pest interactions in (10) is simple and generic, but more advanced interactions can be incorporated that consider. Both for the geometrid moth and the bark beetle case studies, the choice of this simple model provides good agreement between data and model results. This is due to the fact that foliage and bark production in a given year depends on the passage of a pest in the previous year. Notwithstanding the good performance of the stylized model, the limitations of the Lotka-Volterra equations need to be spelled out for the two considered case studies. First, the considered model does not consider intraspecific competition, nor does it include heterogeneity over the landscape due to spatial variation. Also spatial density dependence that considers the increasing number of encounters with hosts that have already been infested, is not included in the current formulation. In fact, in the current model the predator-prey interactions result in cycles of the predator and prey population that are followed indefinitely. In reality, owing to persistent disturbances and changes of the ecosystem, the predator and prey populations would not exhibit regular cycles, but considerably more stochastic behavior. On that account, the predator-prey model should be used with caution, and the model is meaningful mostly for short-term predictions.

Appendix D. Percolation probability through a habitat patch

At the small-scale level, we can derive from the available data the probability β_S that an infestation percolates to the boundaries of a habitat patch. The available fine-scale grid data represents a forest stand as a regular lattice graph, which encourages the use of percolation theory, often applied in the context of disease spread and forest fires. The edges in the lattice graph are marked with a transition probability q, specifying the likelihood that an infested raster cell can contaminate the neighbouring cells within the patch. We model the small-scale infestation rate as $\beta_S = k\theta(q)$, where k encapsulates conditions related to host susceptibility such as tree vigor, or tree size and age effects. The factor $\theta(q)$ is the probability that a pest pervades through the habitat patch, referred to as percolation probability (Grimmett, 1999). Since the percolation probability $\theta(q)$ is hard to obtain analytically as a function of the network size, we resort to simulations considering an $L \times L$ square lattice and approximate the percolation probability by a logistic function as $\theta(q) = 1/(1 + \exp(-k_p(q - q_c)))$, with q_c the critical threshold. The value of q, the likelihood that adjacent grid cells get infested, can be estimated from the available data and is subsequently used to compute $\theta(q)$.

Appendix E. Epidemic threshold in the multi-scale network model

Based on the network dynamics formulated in Eq. (5), we observe that $\mathbf{p}(t) = \mathbf{0}$ is an equilibrium point of Eq. (5), and the asymptotic stability in

the neighbourhood of this stationary point gives rise to the epidemic threshold (Chakrabarti et al., 2008). In order to prove asymptotic stability in a discrete-time system, the eigenvalues of the Jacobian evaluated at the stationary point need to have an absolute value smaller than one. This leads to the necessary conditions of the epidemic threshold in Eq. (1) of the main document (Chakrabarti et al., 2008). The sufficiency of the epidemic threshold can be proven based on the following bound

$$\begin{aligned}\zeta_i(t) &= \prod_{j\in\mathcal{N}_i}(1-\beta_L\beta_S p_j(t-1))\\ &\geq 1-\beta_L\beta_S\sum_{j\in\mathcal{N}_i}p_j(t-1)\,.\end{aligned} \tag{11}$$

Using this bound, we can find a linear approximation of the set of non-linear difference equations (5), which can be written in vector form as

$$\mathbf{p}(t)\leq[\beta_L\beta_S A+(1-\delta)I]\mathbf{p}(t-1)\,. \tag{12}$$

The linearised system is asymptotically stable if the modules of all eigenvalues of the system matrix $S=\beta_L\beta_S A+(1-\delta)I$ are smaller than one, which leads to

$$\frac{\beta_L\beta_S}{\delta}<\frac{1}{\lambda_1(A)}\,, \tag{13}$$

where $\lambda_1(A)$ represents the spectral radius of A, i.e., the supremum of the absolute value of the eigenvalues of A.

Appendix F. Epidemic threshold in a random landscape topology

When the location of all habitat patches is known, the patches can be described by a deterministic network for which the epidemic threshold is given by Eq. (1) of the main document. It is however also relevant to make statistical statements about regions with comparable or rather disparate distance distributions between habitat patches. In this case, we resort to a stochastic characterization by means of a random geometric graph (RGG). In an RGG, the nodes follow a spatial point process, while links are drawn between the nodes that lie within the dispersal range of the pest. The large-scale network can be modelled as the graph $G(\mathcal{V},\mathcal{E})$, with $\mathcal{V}=\{\mathbf{x}_i,\ \mathbf{x}_i\in\Pi_f\}$ where Π_f represents a Poisson point process (PPP) with density μ. The edge set is given by $\mathcal{E}=\{(\mathbf{x}_i,\mathbf{x}_j):\ r=\|\mathbf{x}_i-\mathbf{x}_j\|<R\}$ and R the dispersal capability. The spectral radius of an RGG can be bound by $\lambda_1(A)<l\mu R^2$, with l a positive constant (below). The epidemic threshold in an RGG characterized by the density and the dispersal capability is therefore given by

$$\frac{\beta_L\beta_S}{\delta}<\frac{1}{l\mu R^2}<\frac{1}{\lambda_1(A)}\,. \tag{14}$$

This result illustrates the dependence of the epidemic threshold on the patch density and the dispersal capability, and is important to determine which landscape topologies have high risk for the spread of pests.

Bound on spectral radius of RGG. The bound of the spectral radius can be found based on the sequence of spectral moments (Preciado and Jadbabaie, 2009). To avoid boundary effects in the network, typically a d-dimensional torus is chosen on which the network is laid out. We are interested in Poisson point processes over a square area, and therefore, the constant l has been determined based on simulations $l=2.2247$ (Fig. F.7). The spectral radius is depicted as a function of the expected degree together with an upper bound of the form $\lambda_1(A)<c\mu R^2$ (Fig. F.7). As the expected degree in an RGG is given by $\mathbb{E}[d]=\mu\pi R^2$, the spectral radius is depicted as a function of $\mathbb{E}[d]$. For moderate values of the expected degree, the upper bound is shown to be tight.

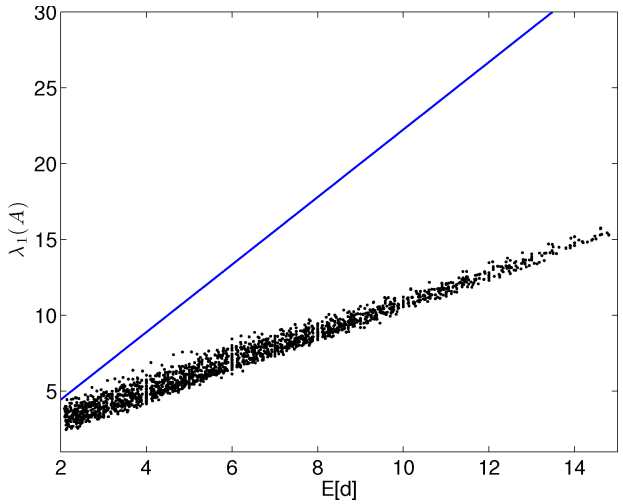

Fig. F.7. Upper bound of the spectral radius of the network adjacency matrix. The dots represent simulated RGGs, whereas the full line represents the upper bound of the spectral radius.

Appendix G. Sensitivity analysis

We present here the sensitivity of the model with respect to the small-scale effects (Fig. G.8). The baseline case uses the following parameters $a_{BL} = -0.81$, $b_{BL} = -4.85$, $c_{BL} = -0.04$ and $d_{BL} = -0.72$. We note that the all parameters of the predator-prey model are negative. This is due to using the available data on infested trees as a proxy for the prey, whereas the fraction of infested trees represents in reality the complement of the prey.

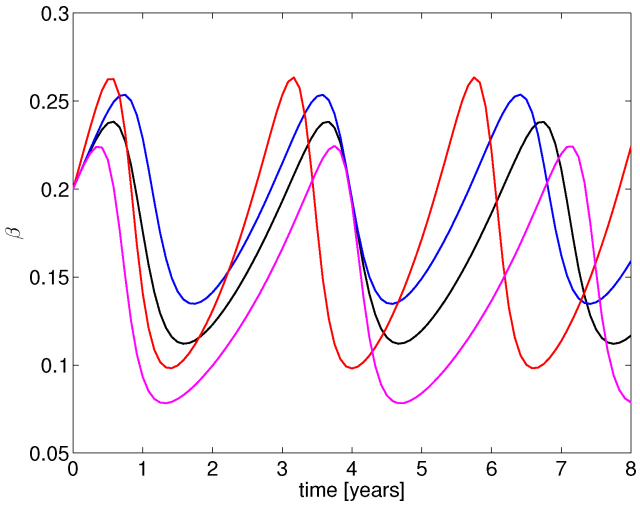

Fig. G.8. Trajectories of the infestation rate β. The baseline case is depicted in black, whereas modification of $a = a_{BL} - 0.1$ is indicated in blue, modification of $c = c_{BL} - 0.02$ is indicated in red, and modification of $b = b_{BL} - 1$ and $d = d_{BL} + 0.1$ is indicated in magenta. We observe that small changes in the parameters lead to substantial changes in the frequency and amplitude of the infestation rate dynamics.

Overview of network parameters and their climate dependency

Table G.1
Illustrative overview of network parameters in the multi-scale pest outbreak framework and their climate dependence. Strong dependence is indicated by $++$, weak dependence by $+$, no dependence by 0.

	Name	Climate dependence	Comments
β	Infestation rate	+	Mainly depends on β_S
β_L	Large-scale infestation rate	+	Only evolves over long time scales with climate variation
β_S	Small-scale infestation rate	++	Varies with inter-annual and seasonal variations in temperature and precipitation
δ	Recovery rate	+	Depends both on annual variations of temperature and precipitations, as well as multi-annual events
γ	Removal rate	+	Depends both on annual variations of temperature and precipitations, as well as multi-annual events
A	Adjacency matrix	0	Virtually no climate influence, except over longer time scales
a, b, c, d	Parameter set of predator-prey dynamics of the Lotka-Volterra equations	++	Varies with inter-annual and seasonal variations in temperature and precipitation
μ	Forest density	0	Virtually no climate influence, except over longer time scales
R	Dispersal capability	0	No demonstrated effect

References

Balcan, D., Colizza, V., Gonçalves, B., Hu, H., Ramasco, J.J., Vespignani, A., 2009. Multiscale mobility networks and the spatial spreading of infectious diseases. Proc. Natl. Acad. Sci. 106 (51), 21484–21489.

Bjørnstad, O.N., Peltonen, M., Liebhold, A.M., Baltensweiler, W., 2002. Waves of larch budmoth outbreaks in the European Alps. Science 298 (5595), 1020–1023.

Brauer, F., Castillo-Chavez, C., 2001. Mathematical Models in Population Biology and Epidemiology, volume 40. Springer.

Cain, M.L., Milligan, B.G., Strand, A.E., 2000. Long-distance seed dispersal in plant populations. Am. J. Bot. 87 (9), 1217–1227.

Carpenter, S.R., 2013. Complex systems: Spatial signatures of resilience. Nature 496 (7445), 308–309.

Chakrabarti, D., Wang, Y., Wang, C., Leskovec, J., Faloutsos, C., 2008. Epidemic thresholds in real networks. ACM Trans. Inform. Syst. Security (TISSEC) 10 (4), 1–26.

Clark, W.C., Jones, D.D., Holling, C.S., 1979. Lessons for ecological policy design: A case study of ecosystem management. Ecolog. Model. 7 (1), 1–53.

Cornelius, S.P., Kath, W.L., Motter, A.E., 2013. Realistic control of network dynamics. Nat. Commun. 4.

Dai, L., Korolev, K.S., Gore, J., 2013. Slower recovery in space before collapse of connected populations. Nature 496 (7445), 355–358.

Dietze, M.C., Matthes, J.H., 2014. A general ecophysiological framework for modelling the impact of pests and pathogens on forest ecosystems. Ecol. Lett. 17 (11), 1418–1426.

Draief, M., Ganesh, A., Massoulié, L., 2008. Thresholds for virus spread on networks. Ann. Appl. Probability 18 (2), 359–378.

Fahse, L., Heurich, M., 2011. Simulation and analysis of outbreaks of bark beetle infestations and their management at the stand level. Ecol. Model. 222 (11), 1833–1846.

Fath, B.D., Patten, B.C., 1999. Review of the foundations of network environ analysis. Ecosystems 2 (2), 167–179.

Fernández, A., Fort, H., 2009. Catastrophic phase transitions and early warnings in a spatial ecological model. J. Stat. Mech. Theor. Exp. P09014.
Finn, J.T., 1976. Measures of ecosystem structure and function derived from analysis of flows. J. Theor. Biol. 56 (2), 363–380.
Gao, J., Buldyrev, S.V., Stanley, H.E., Havlin, S., 2012a. Networks formed from interdependent networks. Nat. Phys. 8 (1), 40.
Gao, J., Buldyrev, S.V., Stanley, H.E., Havlin, S., 2012b. Networks formed from interdependent networks. Nat. Phys. 8 (1), 40.
Gao, J., Li, D., Havlin, S., 2014. From a single network to a network of networks. Natl. Sci. Rev. 1 (3), 346–356.
Grimmett, G.R., 1999. Percolation. Springer.
Haak, D.M., Fath, B.D., Forbes, V.E., Martin, D.R., Pope, K.L., 2017. Coupling ecological and social network models to assess transmission and contagion of an aquatic invasive species. J. Environ. Manag. 190, 243–251.
Hannon, B., 1973. The structure of ecosystems. J. Theor. Biol. 41 (3), 535–546.
Jepsen, J.U., Hagen, S.B., Høgda, K.A., Ims, R.A., Karlsen, S.R., Tømmervik, H., Yoccoz, N.G., 2009a. Monitoring the spatio-temporal dynamics of geometrid moth outbreaks in birch forest using MODIS-NDVI data. Remote Sens. Environ. 113 (9), 1939–1947.
Jepsen, J.U., Hagen, S.B., Karlsen, S.-R., Ims, R.A., 2009b. Phase-dependent outbreak dynamics of geometrid moth linked to host plant phenology. Proc. Roy. Soc. London B Biol. Sci. 4119–4128.
Kautz, M., Meddens, A.J.H., Hall, R.J., Arneth, A., 2017. Biotic disturbances in northern hemisphere forests-a synthesis of recent data, uncertainties and implications for forest monitoring and modelling. Global Ecol. Biogeogr. 26 (5), 533–552.
Keeling, M.J., Eames, K.T., 2005. Networks and epidemic models. J. Roy. Soc. Interface 2 (4), 295–307.
Kermack, W.O., McKendrick, A.G., 1991. Contributions to the mathematical theory of epidemics. Bull. Math. Biol. 53 (1), 33–55.
Lewis, M.A., Nelson, W., Xu, C., 2010. A structured threshold model for mountain pine beetle outbreak. Bull. Math. Biol. 72, 565–589.
Logan, J.A., White, P., Bentz, B.J., Powell, J.A., 1998. Model analysis of spatial patterns in mountain pine beetle outbreaks. Theor. Popul. Biol. 53 (3), 236–255.
Long, J.N., 2009. Emulating natural disturbance regimes as a basis for forest management: a North American view. Forest Ecol. Manag. 257 (9), 1868–1873.
Ludwig, D., Jones, D.D., Holling, C.S., 1978. Qualitative analysis of insect outbreak systems: the spruce budworm and forest. J. Anim. Ecol. 315–332.
Margosian, M.L., Garrett, K.A., Hutchinson, J.M.S., With, K.A., 2009. Connectivity of the american agricultural landscape: assessing the national risk of crop pest and disease spread. Bioscience 59 (2), 141–151.
Meentemeyer, R.K., Haas, S.E., Václavík, T., 2012. Landscape epidemiology of emerging infectious diseases in natural and human-altered ecosystems. Annu. Rev. Phytopathol. 50, 379–402.
Messier, C., Puettmann, K.J., Coates, K.D., 2013. Managing forests as complex adaptive systems: Building resilience to the challenge of global change. Routledge.
Mundt, C.C., Sackett, K.E., Wallace, L.D., Cowger, C., Dudley, J.P., 2009. Long-distance dispersal and accelerating waves of disease: empirical relationships. Am. Nat. 173 (4), 456–466.
Nelson, W.A., Bjørnstad, O.N., Yamanaka, T., 2013. Recurrent insect outbreaks caused by temperature-driven changes in system stability. Science 341 (6147), 796–799.
Newman, M.E.J., 2002. Spread of epidemic disease on networks. Phys. Rev. E 66 (1), 016128.
Pastor-Satorras, R., Vespignani, A., 2001. Epidemic spreading in scale-free networks. Phys. Rev. Lett. 86 (14), 3200–3203.
Pastor-Satorras, R., Vespignani, A., 2002. Epidemic dynamics in finite size scale-free networks. Phys. Rev. E 65 (3), 035108.
Patten, B.C., 1978. Systems approach to the concept of environment. Ohio J. Sci. 78, 206–222.
Peters, D.P.C., Pielke, R.A., Bestelmeyer, B.T., Allen, C.D., Munson-McGee, S., Havstad, K.M., 2004. Cross-scale interactions, nonlinearities, and forecasting catastrophic events. Proc. Natl. Acad. Sci. U. S. A. 101 (42), 15130–15135.
Pocock, M.J., Evans, D.M., Memmott, J., 2012. The robustness and restoration of a network of ecological networks. Science 335 (6071), 973–977.
Preciado, V.M., Jadbabaie, A., 2009. Spectral analysis of virus spreading in random geometric networks. In: In Proceedings of the IEEE Conference on Decision and Control. Shanghai, China. pp. 4802–4807.
Raffa, K.F., Aukema, B.H., Bentz, B.J., Carroll, A.L., Hicke, J.A., Turner, M.G., Romme, W.H., 2008. Cross-scale drivers of natural disturbances prone to anthropogenic amplification: the dynamics of bark beetle eruptions. Bioscience 58 (6), 501–517.
Scheffer, M., Bascompte, J., Brock, W.A., Brovkin, V., Carpenter, S.R., Dakos, V., Held, H., Van Nes, E.H., Rietkerk, M., Sugihara, G., 2009. Early-warning signals for critical transitions. Nature 461 (7260), 53–59.
Seidl, R., 2014. The shape of ecosystem management to come: anticipating risks and fostering resilience. Bioscience 1159–1169.
Seidl, R., Albrich, K., Thom, D., Rammer, W., 2018. Harnessing landscape heterogeneity for managing future disturbance risks in forest ecosystems. J. Environ. Manag. 209, 46–56.
Seidl, R., Donato, D.C., Raffa, K.F., Turner, M.G., 2016a. Spatial variability in tree regeneration after wildfire delays and dampens future bark beetle outbreaks. Proc. Natl. Acad. Sci. 113 (46), 13075–13080.
Seidl, R., Müller, J., Hothorn, T., Bässler, C., Heurich, M., Kautz, M., 2016b. Small beetle, large-scale drivers: how regional and landscape factors affect outbreaks of the european spruce bark beetle. J. Appl. Ecol. 53, 530–540.
Seidl, R., Schelhaas, M.-J., Rammer, W., Verkerk, P.J., 2014. Increasing forest disturbances in Europe and their impact on carbon storage. Nature Climate Change 4 (9), 806–810.
Seidl, R., Thom, D., Kautz, M., Martin-Benito, D., Peltoniemi, M., Vacchiano, G., Wild, J., Ascoli, D., Petr, M., Honkaniemi, J., et al., 2017. Forest disturbances under climate change. Nature Climate Change 7 (6), 395.
Senf, C., Campbell, E.M., Pflugmacher, D., Wulder, M.A., Hostert, P., 2017. A multi-scale analysis of western spruce budworm outbreak dynamics. Landsc. Ecol. 1–14.
Strogatz, S.H., 2001. Exploring complex networks. Nature 410 (6825), 268–276.
Ulanowicz, R.E., 1980. An hypothesis on the development of natural communities. J. Theor. Biol. 85 (2), 223–245.
Urban, D., Keitt, T., 2001. Landscape connectivity: a graph-theoretic perspective. Ecology 82 (5), 1205–1218.
With, K.A., Crist, T.O., 1995. Critical thresholds in species' responses to landscape structure. Ecology 76 (8), 2446–2459.
Zhou, G., Liebhold, A.M., 1995. Forecasting the spatial dynamics of gypsy moth outbreaks using cellular transition models. Landsc. Ecol. 10 (3), 177–189.